Synergistic forcing of the troposphere and stratosphere on explosively developing cyclones over the North Pacific during the cold season

Geophysical Research Letters

RESEARCH LETTER
10.1029/2024GL110069

Key Points:

- The North Pacific explosively developing cyclones during cold season are divided into eight up- and down-ward vertically developing types
- The explosively developing cyclones are proved to be an important link between the stratosphere and troposphere in the mid-high latitudes
- Using the piecewise potential vorticity inversion method, the quantitative forcings on the explosively developing cyclones are explored

Supporting Information:

Supporting Information may be found in the online version of this article.

Correspondence to:

H. Hu,
huhaibo@nju.edu.cn

Citation:

Qian, S., Hu, H., Hodges, K. I., Yang, X.-Q., & Song, T. (2024). Synergistic forcing of the troposphere and stratosphere on explosively developing cyclones over the North Pacific during cold season. *Geophysical Research Letters*, *51*, e2024GL110069. https://doi.org/10.1029/2024GL110069

Received 30 APR 2024
Accepted 21 AUG 2024

Author Contributions:

Visualization: Shengyi Qian, Tangxuan Song
Writing – original draft: Shengyi Qian, Haibo Hu
Writing – review & editing: Haibo Hu, Kevin I. Hodges

Synergistic Forcing of the Troposphere and Stratosphere on Explosively Developing Cyclones Over the North Pacific During Cold Season

Shengyi Qian[1], Haibo Hu[1], Kevin I. Hodges[2], Xiu-Qun Yang[1], and Tangxuan Song[1]

[1]CMA Key Laboratory for Climate Prediction Studies, School of Atmospheric Sciences, Nanjing University, Nanjing, China, [2]Department of Meteorology, University of Reading, Reading, UK

Abstract The mid-latitude extreme weather disasters are often associated with explosively developing cyclones (ECs). Based on different vertical development characteristics, 4,608 ECs identified over the North Pacific in the cold season of 44 years of NCEP-CFSR reanalyzes are divided into four types of upward development and four types of downward development categories. ECs with vertical upward (downward) development follow a northeastward (nearly eastward) path, mainly explosively developing over the Northwest Pacific (Asia continent and Pacific). Furthermore, utilizing the piecewise potential vorticity inversion method reveals the synergetic forcing of the turbulent heat transport and baroclinicity in the lower troposphere, the latent heat release in the middle levels, the upper-level jet stream, and the downward intrusion of stratospheric potential vorticity on the ECs. Different configurations of these influences from the troposphere to the stratosphere result in the occurrences of eight types of ECs in the cold season over the North Pacific.

Plain Language Summary Since the late twentieth century, there has been a significant variation in the frequency of explosively developing cyclones (ECs), which bring extreme weather disasters to the mid-latitudes. This study classifies winter North Pacific ECs into four upward and four downward developing categories. The upward developing ECs include those enhanced only in the lower troposphere (UL-EC), those developing upward to the middle troposphere (UM-EC), those developing upward to the upper troposphere (UU-EC), and those developing upward into the stratosphere (US-EC). In contrast, the downward developing ECs can be classified as those intensifying only in the upper troposphere (DU-EC), those developing downward to the middle troposphere (DM-EC), those developing downward to the lower troposphere (DL-EC), and those developing downward from the stratosphere (DS-EC) to the lower troposphere. Furthermore, the piecewise potential vorticity inversion results show that the explosive development of UL-EC and UM-EC are dominated by the thermodynamical processes in the middle-to-lower troposphere, exhibiting a baroclinic structure with opposite anomalous geopotential height between the troposphere and stratosphere. However, the other types have a consistent stratospheric-to-tropospheric negative anomalies, which is determined by the upper-layer dynamical processes. The downward intrusion of stratospheric potential vorticity dominates the explosive development for the US-EC and DS-EC.

1. Introduction

Extratropical cyclones are defined as locally closed low-pressure systems and are one of the most frequent weather systems in mid-latitudes (Hoskins & Hodges, 2002). Among them, rapidly intensifying extratropical cyclones are known as 'bombs' (Sanders & Gyakum, 1980), which bring about severe extreme weather events in mid-latitudes (Hirata, 2021; Shaw et al., 2016). Extratropical cyclones play an important role in the transport of heat and moisture between low and high latitudes (Peixoto & Oort, 1984). Previous studies show that since the end of the twentieth century, the frequency of explosively developing cyclones (ECs) has a significant variation (Chang, 2014; Ginesta et al., 2022; Iwao et al., 2012; Kuwano-Yoshida et al., 2022). More comprehensive and in-depth research on ECs is necessary.

The North Pacific region is one of the areas where ECs occur frequently, with the most active period during the cold season (November to April) (Alberta et al., 1991; Black & Pezza, 2013; Chen et al., 1992; Kuwano-Yoshida, 2014). Bergeron (1954) was first to give a definition for rapidly deepening extratropical lows. Subsequently, Sanders and Gyakum (1980) quantitatively provided criteria for a 'bomb'. ECs in the Northwest Pacific can be classified into Okhotsk-Japan Sea type, Pacific Ocean-land type, and Pacific Ocean-ocean type

according to their geographical genesis and explosive development locations (Kuwano-Yoshida & Asuma, 2008). The frequency of ECs in the Northern Hemisphere has also been found to be statistically related to the Madden-Julian Oscillation, El Niño-Southern Oscillation, and Quasi-Biennial Oscillation (Attard & Lang, 2019).

The study of ECs dates back to the end of the last century, but there is still much debate about their developmental mechanisms. Baroclinic zones are found to be the most suitable areas for the formation of ECs (Roebber, 1984; Sanders & Gyakum, 1980), and subsequent research has demonstrated the importance of the lower-level baroclinicity in the development of ECs (Anthes et al., 1983; Roebber & Schumann, 2011; Yoshiike & Kawamura, 2009). In addition, numerical experiments by Kuo et al. (1991) emphasized the role of surface heat fluxes, which is confirmed in observational based studies (Gyakum & Danielson, 2000; Neiman & Shapiro, 1993). The elevated surface heat fluxes caused by the sea surface temperature and gradient anomalies are found to significantly impact the occurrence and development of ECs (Bui & Spengler, 2021; Tsopouridis et al., 2021a, 2021b, 2021c). A series of studies by Hirata et al. (2015, 2016, 2018) further revealed the positive feedbacks between the surface heat fluxes and the development of ECs. Significantly, it has become the consensus that latent heat release can also provide developmental energy for ECs (Fosdick & Smith, 1991; Rogers & Bosart, 1991; Strahl & Smith, 2001; Weijenborg & Spengler, 2020; Zhu & Newell, 1994). These studies emphasize that ECs are able to obtain energy from the turbulent heat transport, baroclinicity, and latent heat release in the lower troposphere and then develop upwards.

However, Wash et al. (1992) discovered that some ECs exhibit strong upper-level processes in the initial stage of development, whose characteristics can be statistically separated from non-explosively developing cyclones. Many studies had proved that jet streams and their associated dynamical processes can also contribute to the explosive development of ECs (Chang, 2005; Gilet et al., 2009; Manobianco et al., 1992; Oruba et al., 2013; Rivière & Joly, 2006; Seiler & Zwiers, 2016a, 2016b). The counter propagating Rossby waves perspective of baroclinic instability presented the scenario in which the upper-level potential vorticity (PV) anomalies reinforce the lower-level ones and vice versa (Methven et al., 2005). Using a mesoscale analysis and a simulation system model, Spaete et al. (1994) found there was a net mass transport from the stratosphere to the troposphere overlying the ECs. Subsequently, numerous observational results have confirmed the downward transport of stratospheric PV anomalies during the evolution of ECs (Kang et al., 2020; Pang & Fu, 2017; Reader & Moore, 1995; Wang & Rogers, 2001). In other words, ECs may also derive energy from the upper atmosphere and then develop vertically downwards. Therefore, there is still a considerable debate regarding the vertical development of ECs.

As well as the issue of the vertical development of ECs, there is also uncertainty in the vertical structure of ECs. Lim and Simmonds (2007) considered the vertical structure of mid-latitude cyclones and divided them into shallow-structure and well-organized cyclones. Subsequently, Pepler and Dowdy (2020) further categorized cyclones into the shallow surface cyclone, middle-level cyclone, deep surface cyclone, shallow upper cyclone, and deep upper cyclone. On this basis, Yao et al. (2023) identified differences in the horizontal movement of each category. These studies only focused on the levels below 500 hPa. Nevertheless, cyclones can be found at higher levels. Lakkis et al. (2019, 2021) extended the research levels of mid-latitudes cyclones to the tropopause but did not provide a detailed classification. Thus, we can see that the evolvement mechanism of the ECs with different vertical structures remain unclear.

Motivated by the discussion above, this paper addresses the following key questions: Do ECs with similar vertical structures have the same vertical development processes? What are the vertical development characteristics and classifications of ECs over the North Pacific during the cold season? As reviewed in Spaete et al. (1994), do the strong ECs which link the troposphere and stratosphere always develop downwards from the upper atmosphere? Considering all the potential effects from the troposphere to the stratosphere, what are their quantitative contributions to the vertical development of different ECs? The organization of this paper is as follows: Section 2 introduces the data and methods used in this study, Section 3 presents the classification of ECs with different vertical structures and shows a quantitative analysis and diagnosis of their development mechanisms, and Section 4 provides a summary.

2. Data and Methods

The National Centers for Environmental Prediction (NCEP) Climate Forecast System Reanalysis (CFSR) datasets and its extended Version the Climate Forecast System Version 2 (CFSV2) datasets are used in this study (Saha et al., 2010, 2011) (https://cfs.ncep.noaa.gov/). CFSR provides 6 hourly reanalysis data from 1979 till the present

with a high spatial resolution of 0.5° × 0.5°, and has 37 vertical layers from 1,000 hPa to 1 hPa. The time period of 44 cold seasons (November to April of the following year) from 1979 to 2022 is used for investigation. The high-resolution CFSR reanalysis dataset compares well with other recent high-resolution reanalyzes in cyclone analysis compared to using older low-resolution datasets (Allen et al., 2010; Hodges et al., 2011; Pezza et al., 2016; Roebber et al., 2023).

For the identification of extratropical cyclones, the automatic tracking algorithm by Hodges (1994, 1995, 1996, 1999) is applied. The extratropical cyclones over the North Pacific are traced at the 850 and 300 hPa separately for classifying ECs. The extratropical cyclones are identified as local maxima of relative vorticity (Hoskins & Hodges, 2002). The relevant climatology is subtracted from vorticity field at each time step. The data are first truncated at total wavenumber 42 to remove small-scale noise. Spatial wavenumbers less than or equal to five are also removed to eliminate the influence of the largescale background and a spectral tapering is performed in order to suppress Gibbs phenomena (Hoskins & Sardeshmukh, 1984). A threshold of $1 \times 10^{-5}\ s^{-1}$ is applied to the filtered vorticity to initially identify the feature points. The tracking algorithm is initiated by linking all the feature points based on the nearest neighbor distance between points in subsequent frames so that each feature point is assigned to a track. Then the tracking is performed by minimizing a cost function for the ensemble track smoothness to obtain the minimal set of smoothest tracks (Hodges, 1994, 1999). The track ensembles are filtered based on the choice of the minimum time of existence (1 day, four time steps) and distance moved (10° geodesic, ∼1,000 km). Following the tracking, the sea level pressure (SLP) and geopotential height (GPH) minima at the cyclone center is obtained by bilinear interpolation.

The extratropical cyclones, which are detected at 850 hPa, are considered as an EC if its SLP deepening rate greater than 1 hPa/hr persistent for 12 hr (Sanders & Gyakum, 1980; Yoshida & Asuma, 2004). The SLP deepening rate is calculated as follows (Fu et al., 2020; Gyakum et al., 1989):

$$R_{SLP} = \left(\frac{p_{t-6} - p_{t+6}}{12}\right)\left[\frac{\sin 45^\circ}{\sin\left(\frac{\varphi_{t-6}+\varphi_{t+6}}{2}\right)}\right] \quad (1)$$

where p is the SLP of cyclone center, φ is the latitude of cyclone center and t represents the corresponding time of the cyclone. For cyclones detected at 300 hPa, no criterion has previously been defined as to whether a cyclone has explosively developed. According to hydrostatic balance, the GPH is a valid indicator of cyclonic wind in isobaric coordinates. We can also calculate the GPH deepening rate of 300 hPa similar to Formula 1 to filter ECs at 300 hPa. For simplicity, the threshold of GPH deepening rate for 300 hPa ECs is chosen to the same percentile (29.4% in descending order) of SLP deepening rate threshold (1 hPa/hr) of ECs in all cyclones at 850 hPa. Therefore, we define 8.6 gpm/hr as the explosive threshold for 300 hPa cyclones and a 5% fluctuation of the threshold has no obvious influence on the classification of ECs, which indicates the ECs are not sensitive to the threshold. Figure S1 in Supporting Information S1 (refer to as SI hereafter) illustrates the frequency histogram of deepening rate of ECs and the tracks of ECs show that most ECs explosively develop over the ocean.

The tracked ECs are employed to construct composites of the cyclones. For each EC, a box of size 30° in both latitude and longitude is placed around its center of minimal GPH. The mean system-centered composites of GPH anomaly (deviation from climatology) and its standard deviation at the strongest stage of ECs are presented respectively (Figure S2 in Supporting Information S1). The results show that the maximum GPH variance of both 850 (2,771 cases) and 300 hPa (1,837 cases) occurs at the center of the ECs (the red rectangle of 6° × 6° in Figure S2 in Supporting Information S1), with a regional mean of about −200 gpm. Four specific levels 850, 500, 300, and 100 hPa which respectively correspond to the lower-level, middle-level, upper-level troposphere and stratosphere are selected to estimate the vertical development of ECs. An EC is considered to have developed vertically to that layer if the mean of the GPH anomaly in its central region is less than −200 gpm at a specific level. Therefore, ECs identified at 850 hPa are divided into four upward developing types and ECs identified at 300 hPa are also divided into four downward developing types (Figure 1).

In addition, Rogers and Bosart (1986) divided the lifecycle of ECs into four stages to reveal their development processes. In order to better illustrate the vertical development process of ECs, five representative stages throughout the entire lifetime of ECs are defined: the initial stage (the moment when the cyclone initiates), the

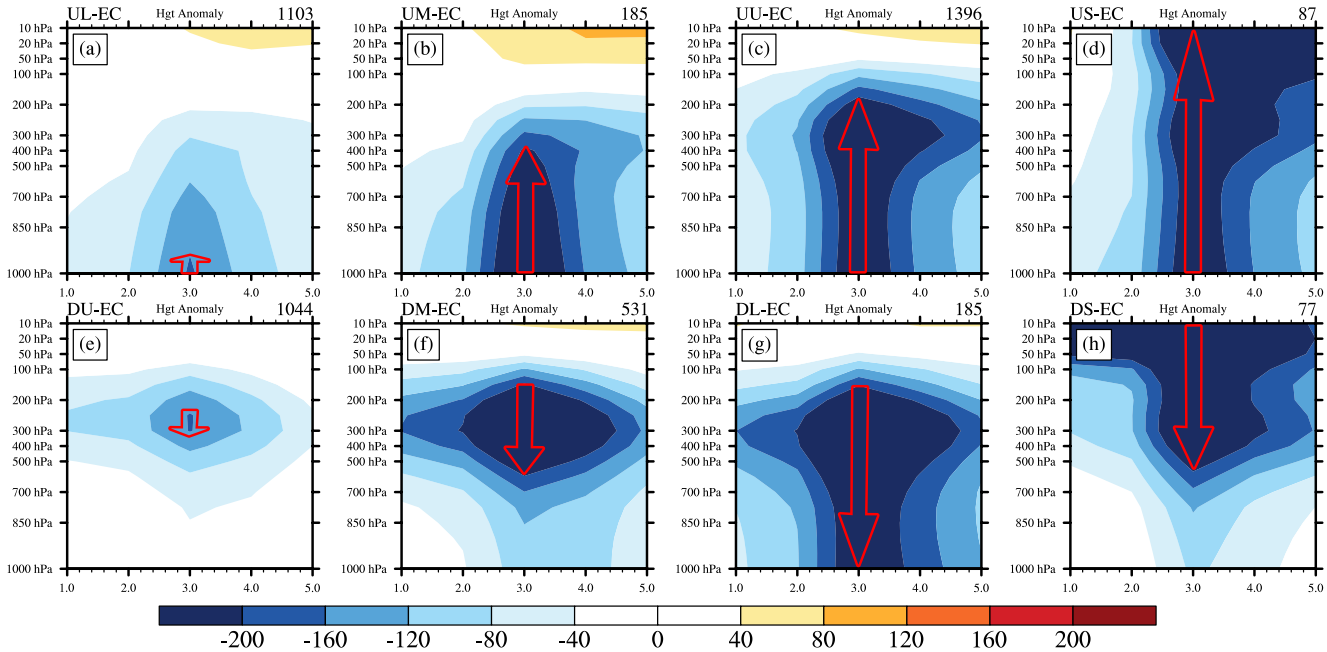

Figure 1. The composites of regional mean of geopotential height anomalies in the ECs' center (shadings, units: gpm) during the 5 representative stages, for the (a) 1,103 cases of ECs that enhanced only in the lower troposphere (UL-EC), (b) 185 cases of ECs that expanding upward to the middle troposphere (UM-EC), (c) 1,396 cases of ECs that expanding upward to the upper troposphere (UU-EC), (d) 87 cases of ECs that expanding upward from the lower troposphere into the stratosphere (US-EC), (e) 1,044 cases of ECs that intensifying only in the upper troposphere (DU-EC), (f) 531 cases of ECs that developing downward to the middle troposphere (DM-EC), (g) 185 cases of ECs that developing downward to the lower troposphere (DL-EC), and (h) 77 cases of ECs that developing downward from the stratosphere (DS-EC) to the lower troposphere. The *x*-axis is the five stages and the *y*-axis is the pressure levels. The direction of red arrows represents the vertical development direction of each ECs type and the length of red arrows indicates the depth of ECs.

explosive development stage (the moment when the ECs reach explosive development), the mature stage (the moment when the central GPH anomalies of ECs are at a minimum), the decay stage (the moment when the central GPH anomalies of ECs increase to the same rate as in the explosive development stage), and the disappearance stage (the moment when the cyclone disappears). Taking UU-EC as an example, the composite GPH anomalies for each stage and the schematic illustration of five stages are shown in Figure S3 in Supporting Information S1.

The piecewise potential vorticity inversion (PPVI) method, which can derive the corresponding GPH by inverting the piecewise PV field, has provided a valid tool for studying ECs (Davis, 1992; Davis & Emanuel, 1991). PPVI is able to quantitatively diagnose the contributions of dynamical and thermodynamical processes to the development of ECs (Dolores-Tesillos et al., 2022; Hirata et al., 2015; Hu et al., 2022; Huo et al., 1999; Milbrandt & Yau, 2001; Seiler, 2019; Tamarin & Kaspi, 2016). Kang and Son (2021) provided a compact linearized PPVI equation. The results of this study are based on this method, with the linearized PPVI equation as follows:

$$q'_n \approx -g\frac{\partial\bar{\theta}}{\partial p}\left[\frac{1}{f}\nabla_p^2\Phi'_n + \frac{f}{\sigma}\frac{\partial^2\Phi'_n}{\partial p^2}\right] \quad (2)$$

Where q is the Ertel potential vorticity, θ is the potential temperature, Φ is the geopotential, g is the gravitational constant, f is the planetary vorticity, $\sigma = -\left(\frac{R_d\pi}{p}\right)\left(\frac{\partial\bar{\theta}}{\partial p}\right)$ where R_d is the gas constant of dry air, $\pi = \left(\frac{p}{p_s}\right)^{R_d/C_p}$ is the Exner function and c_p is the specific heat of dry air under constant pressure. The overbar denotes the time mean, whereas the prime represents the climatological anomaly.

3. Results

Figure 1 illustrates the vertical evolution of eight types of ECs. The composites of the regional mean of GPH anomalies in its center for the five specific lifecycle stages are shown. Among the upward developing ECs, the

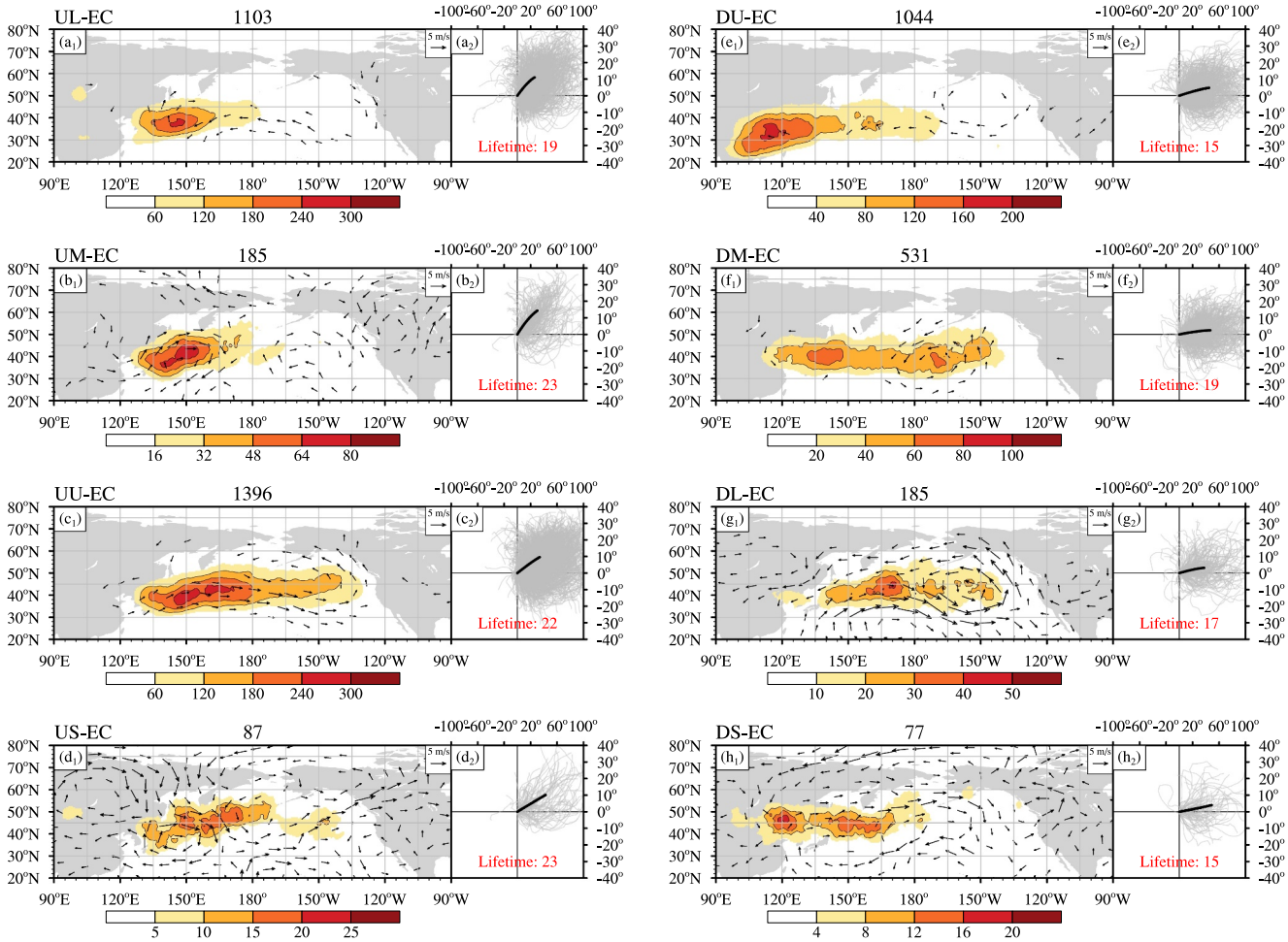

Figure 2. The frequency distribution of where the ECs undergo explosive development (shadings, units: times) and tracks (gray curves) for the (a) UL-EC, (b) UM-EC, (c) UU-EC, (d) US-EC, (e) DU-EC, (f) DM-EC, (g) DL-EC, (h) DS-EC types. The black vectors are wind anomalies (units: m/s) at 300 hPa where only the wind anomalies greater than 2 m/s are drawn. The subscript 1 and 2 of graphic number represent explosive frequency distribution (e.g., a_1) and tracks (e.g., a_2) respectively. The coordinates of all the tracks are relative longitude and latitude. The lifetime (units: 6 hr) of each type is labeled under the mean tracks (black curves).

UU-EC (Figure 1c) is the most prevalent, accounting for 50.4% of all upward developing ECs, followed by UL-EC (Figure 1a) at 39.8%. The UM-EC (Figure 1b) and US-EC (Figure 1d) are the least common, representing 6.7% and 3.1%, respectively. For ECs with downward development, the DU-EC (Figure 1e) is the most common, comprising 56.8% of all downward developing ECs, followed by DM-EC (Figure 1f) at 28.9%. The DL-EC (Figure 1g) and DS-EC (Figure 1h) are the least common, accounting for 10.1% and 4.2%, respectively. The number of UU-EC, UL-EC and DU-EC account for more than 70% of all ECs (Table S1 in Supporting Information S1). It is evident that cyclones generated at lower levels can vertically develop upwards into the upper troposphere or even penetrate through the tropopause into the stratosphere (Figures 1a–1d), while cyclones formed at upper levels can vertically develop downwards into the lower troposphere near the surface, with the existence of stratospheric impact. These findings indicate that there are significant differences in the vertical development of ECs, resulting in distinct vertical structures. Emphasizing solely the forcing of the upper or lower troposphere on the development of ECs is inappropriate. Synergistic forcing of the entire atmosphere, including the stratosphere, needs to be considered.

Figure 2 shows the frequency distribution of where ECs undergo explosive development and tracks of the eight types of ECs. The mean track of ECs is calculated using the least squares method to fit a quadratic function of latitude and longitude relative to time, with the genesis point as the base point. The mean lifetime of each ECs type is used to plot their mean tracks (Gaffney et al., 2007). The upward expanding ECs follow northeastward paths (Figures 2a–2d), while the downward developing ECs follow primarily eastward paths (Figures 2e–2h). The

upward developing ECs are mainly explosively developing over the ocean east of Japan. Importantly, the explosive development locations of US-EC are further north, with some near the Bering Strait, indicating underlying eddy transport from the mid-latitude to the Arctic. In contrast to upward developing ECs, some downward developing ECs explosively develop over the East Asian continent.

The zonal distribution of where the ECs undergo explosive development has two obvious features. On the one hand, the UL-EC and UM-EC (Figures 2a and 2b), that have little signal in the upper troposphere, have a narrower distribution. On the other hand, explosive development locations of other ECs types which extend to the upper troposphere can span almost the complete North Pacific (Figures 2c–2h). From the composite anomaly wind field at 300 hPa, ECs with shallow (deep) vertical structures are accompanied by weaker (stronger) westerly jet streams. Moreover, regarding the genesis of ECs (Figure S4 in Supporting Information S1), the four types of upward ECs, as well as the DU-EC and DS-EC, all overlap with the Western Pacific jet stream and its two upstream branches (Qian et al., 2023). This suggests that the vertical structure of ECs is not only determined by turbulent heat transport, baroclinicity and latent heat release in the lower-middle troposphere but may also be related to upper tropospheric jet streams and even stratospheric PV intrusions. Except for DS-EC, the ECs with deeper structure, which dissipate near the North American continent, have longer lifespans compared to the shallow ones. Shallow ECs at lower and upper levels rapidly decline over the Northwest Pacific and even over the oceanic fronts (Figure S4 in Supporting Information S1).

Based on the introduction, potential forcing factors for the development of ECs include turbulent heat transport and baroclinicity in the lower troposphere, latent heat release in the middle troposphere, jet stream dynamics in the upper troposphere, as well as downward stratospheric PV intrusion. Seiler (2019) categorized the entire PV into three parts at different levels and respectively provided the impacts of turbulent heat transport and baroclinicity, latent heat release, and downward stratospheric PV intrusion. To further differentiate the impacts of upper-level jet stream activity and stratospheric PV intrusion in the PPVI method, we divide PV into pieces that are related to turbulent heat transport and baroclinicity (q_{flux}, 1,000, 950, and 900 hPa), latent heat release (q_{dia}, 850, 800, 700, 600, and 500 hPa), upper-level jet streams (q_{jet}, 400, 300, 250, and 200 hPa), and stratospheric PV effects (q_{str}, 150, 100, 50, 20, and 10 hPa). Horizontally, the domain spans ±30° zonally and ±15° meridionally about the ECs center. Due to the sufficiently wide horizontal domain, the influence of the lateral boundary condition can be ignored. The Dirichlet boundary condition is applied at the lateral boundaries and Neumann boundary conditions are applied to the vertical boundaries. The inverted vertical evolution results of ECs are consistent with observations, and the contributions of each PV piece to the development of ECs are significantly different (Figures S5 and S6 in Supporting Information S1).

To compare the impacts of various forcing factors on the ECs more directly, we calculate the vertical average inversion results at different levels and plot the vertical average results at the mature stage of the ECs (Figure 3). The results indicate that the development of the UL-EC is mainly caused by turbulent heat transport and baroclinicity and latent heat release. These two factors account for 85% of the total GPH changes (Figure 3a), with the role of latent heat release being more significant (43%). The UM-EC that explosively expand upward to higher levels are dominated by latent heat release accounting for 49% of the total GPH changes (Figure 3b). The upward expansion of the UU-EC in Figure 3c occurs throughout the whole troposphere and is predominantly driven by the contribution from the upper-level jet stream (accounting for 72% in the upper levels). It is noteworthy that the negligible middle and upper-level GPH anomalies in the UL-EC and the UM-EC are also influenced by the jet stream. Meanwhile, the impact of the jet stream on the UU-EC is able to propagate downwards to the lower atmosphere. Compared to the other three types of upward developing ECs, the stratospheric PV significantly affects the total GPH anomalies of the US-EC (Figure 3d). Particularly within the stratosphere of the US-EC, the proportion of GPH changes caused by the stratospheric PV reaches 94% of total anomalies. However, the impacts of the jet stream, latent heat release, and turbulent heat transport and baroclinicity contributions are non-negligible in the middle and lower troposphere of the US-EC. The vertical structures of the four upward developing ECs, as well as the US-EC and the UU-EC, are determined by the upper-level dynamical processes, exhibiting a consistent negative anomaly in the total anomalous GPH fields. In contrast, the UM-EC and the UL-EC, dominated by mid-to-lower-level thermodynamical processes, display a baroclinic structure where the anomalous GPH fields are opposite between lower and upper level.

For the downward developing ECs, the DU-EC experiences explosive development mainly in the upper levels, with the GPH decrease predominantly caused by the upper-level jet stream accounting for 76% of the total GPH

10.1029/2024GL110069

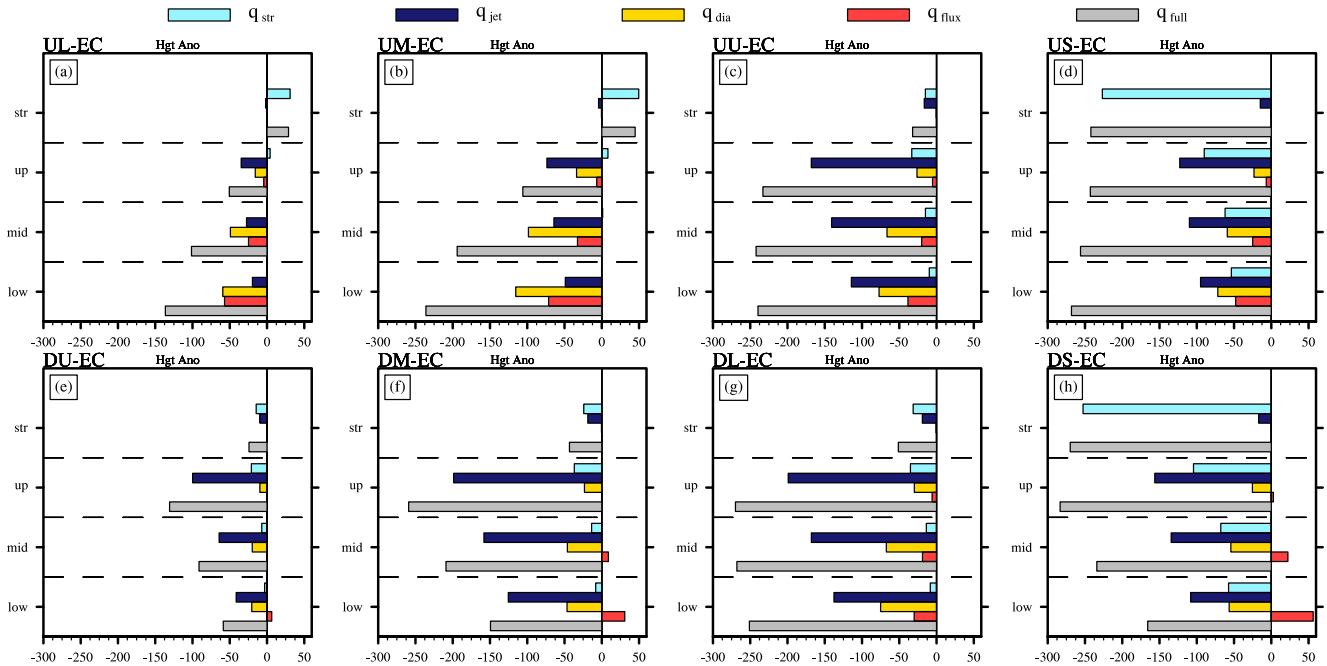

Figure 3. The mean of geopotential height anomalies inverted from the piecewise potential vorticity at different levels for the mature stage. The red bars represent the inversion results of PV associated with turbulent heat transport and baroclinicity in the lower-level (q_{flux}). The gold bars represent the inversion results of PV associated with latent heat release in the mid-level (q_{dia}). The blue bars represent the inversion results of PV associated with jet stream in the upper-level (q_{jet}). The sky-blue bars represent the inversion results of stratospheric PV (q_{str}). And the gray bars represent the inversion results of full PV (q_{full}). The y-coordinates labeled low, mid, up, and str indicate the mean of the geopotential height anomalies obtained from inverted piecewise PV in the 1,000–850 hPa, 850–500 hPa, 500–200 hPa, and 200–10 hPa height bands. The x-coordinates are the value of geopotential height anomalies (units: gpm).

changes (Figure 3e). For the DM-EC, development occurs from upper-level to mid-level, and is still primarily influenced by the jet stream (77%). However, compared to the DU-EC, the DM-EC exhibits stronger latent heat release, but the turbulent heat transport and baroclinicity inhibit its further downward development (Figure 3f). Similar to the UU-EC, the DL-EC also experiences explosive development throughout the troposphere, but DL-EC develops downwards from the upper levels to the middle levels (Figure 3g). The impact of the jet stream remains the most critical factor in the explosive development of the DL-EC (64%). In contrast, the turbulent heat transport and baroclinicity in the mid-to-lower troposphere play a significant role in the downward development of the DL-EC accompanied by the largest positive contributions of latent heat release in all downward developing types. For the DS-EC, similar to the US-EC, is significantly influenced by stratospheric PV throughout its vertical structure. In the stratosphere of the DS-EC, the downward intrusion of stratospheric PV results in a GPH decreases which exceeds 90% of the total anomalies (Figure 3h). The impact of the jet stream dynamics (59%) is more important for the development of the US-EC within the troposphere, and latent heat release also somewhat promotes its downward development. But the turbulent heat transport and baroclinicity in the lower-level act as inhibiting factors for the US-EC. The four downward developing ECs are all dominated by upper-level dynamical processes, and the GPH shows consistent negative anomalies. More importantly, the sign of contributions from the turbulent heat transport and baroclinicity determines whether they can ultimately develop downwards to the surface.

The three-dimensional structural features and vertical tilt of these ECs are also demonstrated in Figure 4. Regarding the two types of ECs related to the stratosphere, the stratospheric GPH anomalies in the US-EC and the DS-EC exhibit a more pronounced northward tilt. The different types of ECs may have the same vertical structure (UL-EC and DU-EC, UM-EC and EM-EC, UU-EC and DL-EC, US-EC and DS-EC), but their vertical development direction and mechanisms are totally different.

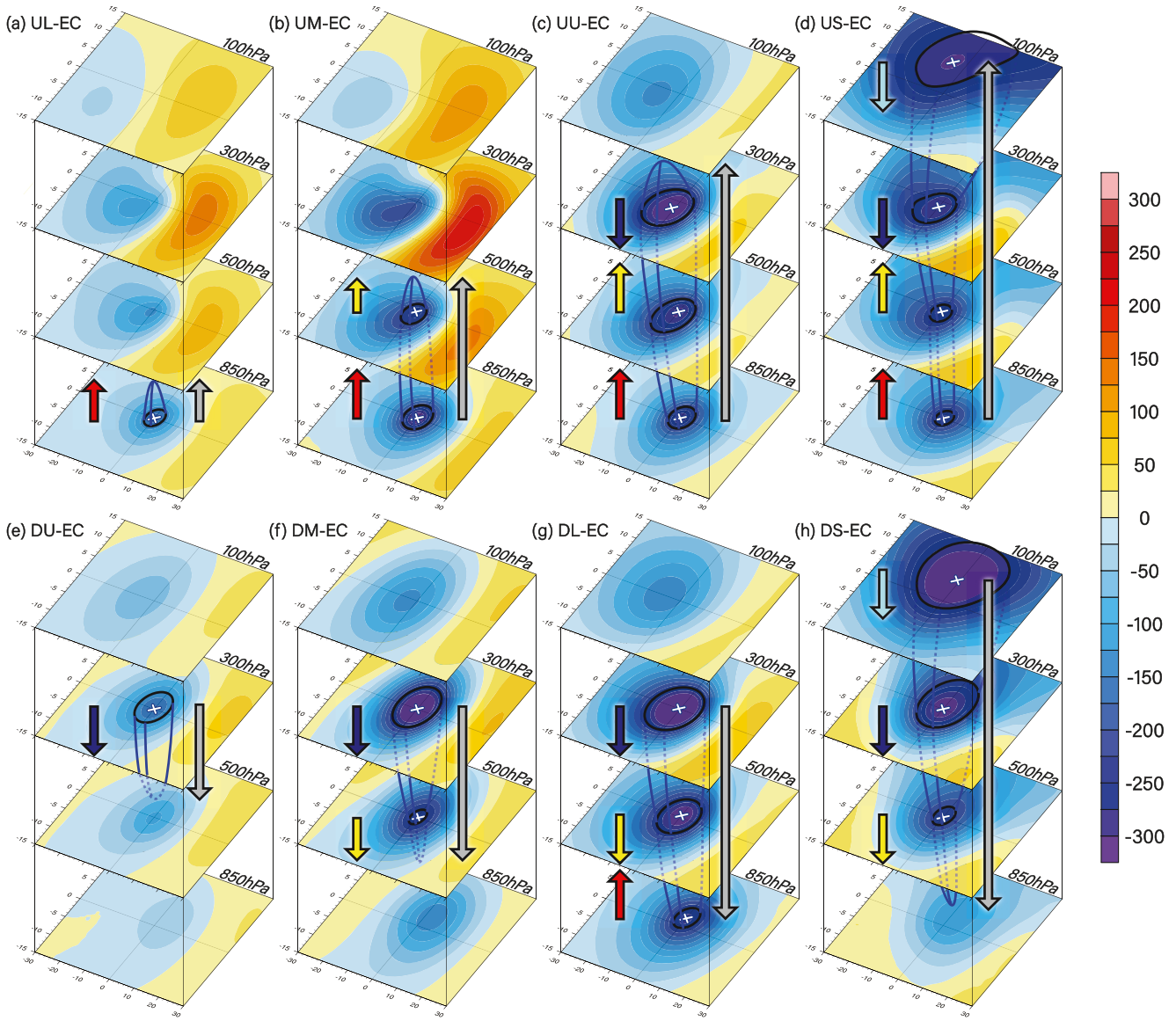

Figure 4. The three-dimensional structure and schematic illustration of development mechanism of eight types of ECs. (a) The fields from top to bottom are composites of system-centered geopotential height anomalies (shadings, units: gpm) of UL-EC at 100, 300, 500, and 850 hPa respectively where the coordinates are the relative longitude and latitude. (b)–(h) are similar to (a), but for UM-EC, UU-EC, US-EC, DU-EC, DM-EC, DL-EC, and DS-EC respectively. The dashed lines of the 0° in latitude and longitude (i.e., the origin of coordinates) is the vorticity center at 850 hPa in (a)–(d), while the vorticity centers in (e)–(h) are located at 300 hPa. The red, gold, blue, and sky-blue arrows represent the impacts of turbulent heat transport, latent heat release, jet stream, and stratospheric PV respectively, and the direction of the arrows shows the propagation direction of impacts. The gray arrows represent the vertical development direction of ECs. The white symbols of 'x' denote the minima of geopotential height anomalies and the bold black cycles present the large value region of geopotential height anomalies at each level.

4. Conclusions

Explosive cyclones (ECs) can lead to extreme weather impacts in the mid-latitudes, with the frequency of ECs seen to has a significant variation since the late twentieth century. However, current understanding of the vertical structure and development mechanisms of ECs remains uncertain. In this study, we utilize the 6-hourly high-resolution CFSR reanalysis data of 44 cold season to identify and track 4,608 ECs occurring at the lower and upper troposphere over the North Pacific. Based on their vertical evolution features, the ECs are further divided into four types of upward and four types of downward developing cyclones. The upward developing ECs include those enhanced only in the lower troposphere (UL-EC), those developing upward to the middle troposphere (UM-EC), those developing upward to the upper troposphere (UU-EC), and those developing upward into the

stratosphere (US-EC). In contrast, the downward developing ECs can be classified as those intensifying only in the upper troposphere (DU-EC), those developing downward to the middle troposphere (DM-EC), those developing downward to the lower troposphere (DL-EC), and those developing downward from the stratosphere (DS-EC) to the lower troposphere. Among all types of ECs, the most prevalent type of ECs is the UU-EC (30.3% of all ECs) that originate in the lower troposphere and expand upward to the tropopause. Meanwhile, the DU-EC (22.7% of all ECs) which intensify only in the upper troposphere are the largest proportion of the downward developing ECs. This indicates that during the cold season, ECs generated at lower levels can mostly explosively develop upward to the upper troposphere after passing over the North Pacific Ocean, while ECs formed in the upper troposphere require more stringent conditions for their downward intensification. The mean track reveals that the paths of upward developing ECs are generally northeastward, with their explosive locations mainly over the Northwest Pacific. On the other hand, the paths of downward developing ECs are nearly eastward, with some explosively developing over the Eurasian continent and others over the Northwest Pacific. The ECs with deeper vertical structure are associated with stronger upper-level jet streams and have a wider zonal distribution of explosive development locations. Additionally, concerning the generation locations, the ECs in the North Pacific are likely related to the polar front jet stream and subtropical jet stream over the Eurasian continent (Chen et al., 2020; Qian et al., 2023). Deep ECs with longer lifetimes can reach North America. In contrast, shallow ECs at lower and upper levels rapidly weaken over the North Pacific, and even disappear over the oceanic fronts in the Northwest Pacific.

Piecewise potential vorticity inversion reveals that the development of ECs forced by the entire atmosphere, including the stratosphere. For upward developing ECs, the explosive development of UL-EC and UM-EC is primarily dominated by latent heat release in the middle troposphere, exhibiting a baroclinic structure of geopotential height anomalies with opposite signs between upper and lower levels. However, the forcing from turbulent heat transport and baroclinicity in the lower troposphere for the UL-EC (29%) is stronger than that for the UM-EC (15%). The UU-EC and US-EC, as well as the four types of downward ECs, are dominated by the upper-level dynamical processes of the jet stream, exhibiting a consistent negative anomalies in geopotential height from the troposphere to the stratosphere. Although the UU-EC expands upward from the lower troposphere, it is worth noting that the most significant enhancement of UU-EC is achieved by the downward influence of the upper-level jet streams. In the case of US-EC, excepting the effect of the jet stream, the impact of stratospheric PV on the total geopotential height anomalies is also crucial, especially within the stratosphere. Moreover, the contributions of latent heat release, turbulent heat transport, and baroclinicity at lower levels are important for the tropospheric development of US-EC. The latent heat release impacts on the downward developing ECs, that is, DU-EC, DM-EC, and DS-EC, are relatively weak. Furthermore, the DU-EC, DM-EC, and DS-EC are even suppressed by the turbulent heat transport and baroclinicity at the lower levels. Nevertheless, the DL-EC expands from the upper troposphere to the lower troposphere accompanied by the positive contributions from the latent heat release, the turbulent heat transport, and baroclinicity in the lower troposphere. Similar to the US-EC, the downward intrusion of stratospheric PV affects the entire vertical development of the DS-EC.

In summary, this study categorizes ECs based on their vertical development characteristics and reveals their respective development mechanisms. Moreover, the cyclone can be influenced by large scale background mean state such as mid-latitude Rossby waves or the perturbation from the tropics (Sun et al., 2024; Yang et al., 2023), which should be considered in the future studies. The weather and climate impacts of these ECs deserve further discussion, which are important for improving winter weather forecasting and meteorological disaster warning in the middle and high latitudes.

Conflict of Interest

The authors declare no conflicts of interest relevant to this study.

Data Availability Statement

The observational data sets used in our study are the NCEP Climate Forecast System Reanalysis 6-hourly data (Saha et al., 2010) and its extension version of Climate Forecast System version 2 (Saha et al., 2011) are able to download from https://rda.ucar.edu/.

Acknowledgments
We are very grateful the technical support from Huyang (Institute of Heavy Rain, China Meteorological Administration, Wuhan), Christian Seiler (Queen's University), Talia Tamarin-Brodsky (Massachusetts Institute of Technology), Christopher A. Davis (National Center of Atmospheric Research), and Edgar Dolores-Tesillos (University of Bern). This work was supported by the National Key Program for developing Basic Science (Grants 2022YFF0801702 and 2022YFE0106600), the National Natural Science Foundation of China (Grants 42175060), and the Jiangsu Province Science Foundation (Grant BK20201259). The authors are thankful for the support of the Jiangsu Provincial Innovation Center for Climate Change.

References

Alberta, T. L., Colucci, S. J., & Davenport, J. C. (1991). Rapid 500-mb cyclogenesis and anticyclogenesis. *Monthly Weather Review*, *119*(5), 1186–1204. https://doi.org/10.1175/1520-0493(1991)119<1186:Rmcaa>2.0.Co;2

Allen, J. T., Pezza, A. B., & Black, M. T. (2010). Explosive cyclogenesis: A global climatology comparing multiple reanalyses. *Journal of Climate*, *23*(24), 6468–6484. https://doi.org/10.1175/2010jcli3437.1

Anthes, R. A., Kuo, Y. H., & Gyakum, J. R. (1983). Numerical simulations of a case of explosive marine cyclogenesis. *Monthly Weather Review*, *111*(6), 1174–1188. https://doi.org/10.1175/1520-0493(1983)111<1174:Nsoaco>2.0.Co;2

Attard, H. E., & Lang, A. L. (2019). The impact of tropospheric and stratospheric tropical variability on the location, frequency, and duration of cool-season extratropical synoptic events. *Monthly Weather Review*, *147*(2), 519–542. https://doi.org/10.1175/Mwr-D-18-0039.1

Bergeron, T. (1954). Review of modern meteorology—12. The problem of tropical hurricanes. *Quarterly Journal of the Royal Meteorological Society*, *80*(344), 131–164. https://doi.org/10.1002/qj.49708034402

Black, M. T., & Pezza, A. B. (2013). A universal, broad-environment energy conversion signature of explosive cyclones. *Geophysical Research Letters*, *40*(2), 452–457. https://doi.org/10.1002/grl.50114

Bui, H., & Spengler, T. (2021). On the influence of sea surface temperature distributions on the development of extratropical cyclones. *Journal of the Atmospheric Sciences*, *78*(4), 1173–1188. https://doi.org/10.1175/Jas-D-20-0137.1

Chang, E. K. M. (2005). The impact of wave packets propagating across Asia on Pacific cyclone development. *Monthly Weather Review*, *133*(7), 1998–2015. https://doi.org/10.1175/Mwr2953.1

Chang, E. K. M. (2014). Impacts of background field removal on CMIP5 projected changes in Pacific winter cyclone activity. *Journal of Geophysical Research-Atmospheres*, *119*(8), 4626–4639. https://doi.org/10.1002/2013jd020746

Chen, F. F., Chen, Q. Y., Hu, H. B., Fang, J. B., & Bai, H. K. (2020). Synergistic effects of midlatitude atmospheric upstream disturbances and oceanic subtropical front intensity variability on western pacific jet stream in winter. *Journal of Geophysical Research-Atmospheres*, *125*(17). https://doi.org/10.1029/2020JD032788

Chen, S. J., Kuo, Y. H., Zhang, P. Z., & Bai, Q. F. (1992). Climatology of explosive cyclones off the East-asian coast. *Monthly Weather Review*, *120*(12), 3029–3035. https://doi.org/10.1175/1520-0493(1992)120<3029:Coecot>2.0.Co;2

Davis, C. A. (1992). Piecewise potential vorticity inversion. *Journal of the Atmospheric Sciences*, *49*(16), 1397–1411. https://doi.org/10.1175/1520-0469(1992)049<1397:Ppvi>2.0.Co;2

Davis, C. A., & Emanuel, K. A. (1991). Potential vorticity diagnostics of cyclogenesis. *Monthly Weather Review*, *119*(8), 1929–1953. https://doi.org/10.1175/1520-0493(1991)119<1929:Pvdoc>2.0.Co;2

Dolores-Tesillos, E., Teubler, F., & Pfahl, S. (2022). Future changes in North Atlantic winter cyclones in CESM-LE - Part 1: Cyclone intensity, potential vorticity anomalies, and horizontal wind speed. *Weather and Climate Dynamics*, *3*(2), 429–448. https://doi.org/10.5194/wcd-3-429-2022

Fosdick, E. K., & Smith, P. J. (1991). Latent-heat release in an extratropical cyclone that developed explosively over the southeastern united-states. *Monthly Weather Review*, *119*(1), 193–207. https://doi.org/10.1175/1520-0493(1991)119<0193:Lhriae>2.0.Co;2

Fu, G., Sun, Y., Sun, J., & Li, P. (2020). A 38-year climatology of explosive cyclones over the northern Hemisphere. *Advances in Atmospheric Sciences*, *37*(2), 143–159. https://doi.org/10.1007/s00376-019-9106-x

Gaffney, S. J., Robertson, A. W., Smyth, P., Camargo, S. J., & Ghil, M. (2007). Probabilistic clustering of extratropical cyclones using regression mixture models. *Climate Dynamics*, *29*(4), 423–440. https://doi.org/10.1007/s00382-007-0235-z

Gilet, J. B., Plu, M., & Rivière, G. (2009). Nonlinear baroclinic dynamics of surface cyclones crossing a zonal jet. *Journal of the Atmospheric Sciences*, *66*(10), 3021–3041. https://doi.org/10.1175/2009jas3086.1

Ginesta, M., Yiou, P., Messori, G., & Faranda, D. (2022). A methodology for attributing severe extratropical cyclones to climate change based on reanalysis data: The case study of storm alex 2020. *Climate Dynamics*, *61*(1–2), 229–253. https://doi.org/10.1007/s00382-022-06565-x

Gyakum, J. R., Anderson, J. R., Grumm, R. H., & Gruner, E. L. (1989). North pacific cold-season surface cyclone activity: 1975–1983. *Monthly Weather Review*, *117*(6), 1141–1155. https://doi.org/10.1175/1520-0493(1989)117<1141:NPCSSC>2.0.CO;2

Gyakum, J. R., & Danielson, R. E. (2000). Analysis of meteorological precursors to ordinary and explosive cyclogenesis in the Western North Pacific. *Monthly Weather Review*, *128*(3), 851–863. https://doi.org/10.1175/1520-0493(2000)128<0851:Aompto>2.0.Co;2

Hirata, H. (2021). Climatological features of strong winds caused by extratropical cyclones around Japan. *Journal of Climate*, *34*(11), 4481–4494. https://doi.org/10.1175/Jcli-D-20-0577.1

Hirata, H., Kawamura, R., Kato, M., & Shinoda, T. (2015). Influential role of moisture supply from the kuroshio/kuroshio extension in the rapid development of an extratropical cyclone. *Monthly Weather Review*, *143*(10), 4126–4144. https://doi.org/10.1175/Mwr-D-15-0016.1

Hirata, H., Kawamura, R., Kato, M., & Shinoda, T. (2016). Response of rapidly developing extratropical cyclones to sea surface temperature variations over the western Kuroshio-Oyashio confluence region. *Journal of Geophysical Research-Atmospheres*, *121*(8), 3843–3858. https://doi.org/10.1002/2015jd024391

Hirata, H., Kawamura, R., Kato, M., & Shinoda, T. (2018). A positive feedback process related to the rapid development of an extratropical cyclone over the kuroshio/kuroshio extension. *Monthly Weather Review*, *146*(2), 417–433. https://doi.org/10.1175/Mwr-D-17-0063.1

Hodges, K. I. (1994). A general-method for tracking analysis and its application to meteorological data. *Monthly Weather Review*, *122*(11), 2573–2586. https://doi.org/10.1175/1520-0493(1994)122<2573:Agmfta>2.0.Co;2

Hodges, K. I. (1995). Feature tracking on the unit-sphere. *Monthly Weather Review*, *123*(12), 3458–3465. https://doi.org/10.1175/1520-0493(1995)123<3458:Ftotus>2.0.Co;2

Hodges, K. I. (1996). Spherical nonparametric estimators applied to the UGAMP model integration for AMIP. *Monthly Weather Review*, *124*(12), 2914–2932. https://doi.org/10.1175/1520-0493(1996)124<2914:Sneatt>2.0.Co;2

Hodges, K. I. (1999). Adaptive constraints for feature tracking. *Monthly Weather Review*, *127*(6), 1362–1373. https://doi.org/10.1175/1520-0493(1999)127<1362:Acfft>2.0.Co;2

Hodges, K. I., Lee, R. W., & Bengtsson, L. (2011). A comparison of extratropical cyclones in recent reanalyses ERA-interim, NASA MERRA, NCEP CFSR, and JRA-25. *Journal of Climate*, *24*(18), 4888–4906. https://doi.org/10.1175/2011jcli4097.1

Hoskins, B. J., & Hodges, K. I. (2002). New perspectives on the Northern Hemisphere winter storm tracks. *Journal of the Atmospheric Sciences*, *59*(6), 1041–1061. https://doi.org/10.1175/1520-0469(2002)059<1041:Npotnh>2.0.Co;2

Hoskins, B. J., & Sardeshmukh, P. D. (1984). Spatial smoothing on the sphere. *Monthly Weather Review*, *112*(12), 2524–2529. https://doi.org/10.1175/1520-0493(1984)112<2524:Ssots>2.0.Co;2

Hu, Y., Deng, Y., Lin, Y. L., Zhou, Z. M., Cui, C. G., Li, C., & Dong, X. Q. (2022). Indirect effect of diabatic heating on Mei-yu frontogenesis. *Climate Dynamics*, *59*(3–4), 851–868. https://doi.org/10.1007/s00382-022-06159-7

Huo, Z., Zhang, D.-L., & Gyakum, J. R. (1999). Interaction of potential vorticity anomalies in extratropical cyclogenesis. Part I: Static piecewise inversion. *Monthly Weather Review*, *127*(11), 2546–2562. https://doi.org/10.1175/1520-0493(1999)127<2546:IOPVAI>2.0.CO;2

Iwao, K., Inatsu, M., & Kimoto, M. (2012). Recent changes in explosively developing extratropical cyclones over the winter northwestern pacific. *Journal of Climate*, *25*(20), 7282–7296. https://doi.org/10.1175/Jcli-D-11-00373.1

Kang, J. M., Lee, J., Son, S. W., Kim, J., & Chen, D. L. (2020). The rapid intensification of East Asian cyclones around the Korean peninsula and their surface impacts. *Journal of Geophysical Research-Atmospheres*, *125*(2). https://doi.org/10.1029/2019JD031632

Kang, J. M., & Son, S. W. (2021). Development processes of the explosive cyclones over the Northwest Pacific: Potential vorticity tendency inversion. *Journal of the Atmospheric Sciences*, *78*(6), 1913–1930. https://doi.org/10.1175/Jas-D-20-0151.1

Kuo, Y. H., Reed, R. J., & Lownam, S. (1991). Effects of surface-energy fluxes during the early development and rapid intensification stages of 7 explosive cyclones in the western atlantic. *Monthly Weather Review*, *119*(2), 457–476. https://doi.org/10.1175/1520-0493(1991)119<0457:Eosefd>2.0.Co;2

Kuwano-Yoshida, A. (2014). Using the local deepening rate to indicate extratropical cyclone activity. *Sola*, *10*(0), 199–203. https://doi.org/10.2151/sola.2014-042

Kuwano-Yoshida, A., & Asuma, Y. (2008). Numerical study of explosively developing extratropical cyclones in the northwestern pacific region. *Monthly Weather Review*, *136*(2), 712–740. https://doi.org/10.1175/2007mwr2111.1

Kuwano-Yoshida, A., Okajima, S., & Nakamura, H. (2022). Rapid increase of explosive cyclone activity over the midwinter North Pacific in the late 1980s. *Journal of Climate*, *35*(3), 1113–1133. https://doi.org/10.1175/Jcli-D-21-0287.1

Lakkis, S. G., Canziani, P., Yuchechen, A., Rocamora, L., Caferri, A., Hodges, K., & O'Neill, A. (2019). A 4D feature-tracking algorithm: A multidimensional view of cyclone systems. *Quarterly Journal of the Royal Meteorological Society*, *145*(719), 395–417. https://doi.org/10.1002/qj.3436

Lakkis, S. G., Canziani, P. O., Rodriguez, J. O., Yuchechen, A. E., O'Neill, A., Albers, K. H., & Hodges, K. (2021). Early 21st century cyclone climatology: A 3D perspective.Basic characterization. *International Journal of Climatology*, *41*(7), 4019–4046. https://doi.org/10.1002/joc.7056

Lim, E.-P., & Simmonds, I. (2007). Southern Hemisphere winter extratropical cyclone characteristics and vertical organization observed with the ERA-40 data in 1979–2001. *Journal of Climate*, *20*(11), 2675–2690. https://doi.org/10.1175/JCLI4135.1

Manobianco, J., Uccelini, L. W., Brill, K. F., & Kuo, Y. H. (1992). The impact of dynamic data assimilation on the numerical simulations of the qe-ii cyclone and an analysis of the jet streak influencing the precyclogenetic environment. *Monthly Weather Review*, *120*(9), 1973–1996. https://doi.org/10.1175/1520-0493(1992)120<1973:Tiodda>2.0.Co;2

Methven, J., Heifetz, E., Hoskins, B. J., & Bishop, C. H. (2005). The counter-propagating Rossby-wave perspective on baroclinic instability. Part III: Primitive-equation disturbances on the sphere. *Quarterly Journal of the Royal Meteorological Society*, *131*(608), 1393–1424. https://doi.org/10.1256/qj.04.22

Milbrandt, J. A., & Yau, M. K. (2001). A mesoscale modeling study of the 1996 Saguenay flood. *Monthly Weather Review*, *129*(6), 1419–1440. https://doi.org/10.1175/1520-0493(2001)129<1419:Ammsot>2.0.Co;2

Neiman, P. J., & Shapiro, M. A. (1993). The life-cycle of an extratropical marine cyclone.1. Frontal-cyclone evolution and thermodynamic air-sea interaction. *Monthly Weather Review*, *121*(8), 2153–2176. https://doi.org/10.1175/1520-0493(1993)121<2153:Tlcoae>2.0.Co;2

Oruba, L., Lapeyre, G., & Rivière, G. (2013). On the poleward motion of midlatitude cyclones in a baroclinic meandering jet. *Journal of the Atmospheric Sciences*, *70*(8), 2629–2649. https://doi.org/10.1175/Jas-D-12-0341.1

Pang, H. J., & Fu, G. (2017). Case study of potential vorticity tower in three explosive cyclones over eastern asia. *Journal of the Atmospheric Sciences*, *74*(5), 1445–1454. https://doi.org/10.1175/Jas-D-15-0330.1

Peixoto, J. P., & Oort, A. H. (1984). Physics of climate. *Reviews of Modern Physics*, *56*(3), 365–429. https://doi.org/10.1103/revmodphys.56.365

Pepler, A., & Dowdy, A. (2020). A three-dimensional perspective on extratropical cyclone impacts. *Journal of Climate*, *33*(13), 5635–5649. https://doi.org/10.1175/Jcli-D-19-0445.1

Pezza, A., Sadler, K., Uotila, P., Vihma, T., Mesquita, M. D. S., & Reid, P. (2016). Southern Hemisphere strong polar mesoscale cyclones in high-resolution datasets. *Climate Dynamics*, *47*(5–6), 1647–1660. https://doi.org/10.1007/s00382-015-2925-2

Qian, S. Y., Hu, H. B., Ren, X. J., Yang, X. Q., Yu, P. L., & Mao, K. F. (2023). Synergistic effects of upstream disturbances and oceanic fronts on the subseasonal evolution of western pacific jet stream in winter. *Journal of Geophysical Research-Atmospheres*, *128*(17). https://doi.org/10.1029/2022JD038331

Reader, M. C., & Moore, G. W. K. (1995). Stratosphere-troposphere interactions associated with a case of explosive cyclogenesis in the labrador-sea. *Tellus Series a-Dynamic Meteorology and Oceanography*, *47*(5), 849–863. https://doi.org/10.1034/j.1600-0870.1995.00124.x

Rivière, G., & Joly, A. (2006). Role of the low-frequency deformation field on the explosive growth of extratropical cyclones at the jet exit. Part I: Barotropic critical region. *Journal of the Atmospheric Sciences*, *63*(8), 1965–1981. https://doi.org/10.1175/Jas3728.1

Roebber, P. J. (1984). Statistical-analysis and updated climatology of explosive cyclones. *Monthly Weather Review*, *112*(8), 1577–1589. https://doi.org/10.1175/1520-0493(1984)112<1577:Saauco>2.0.Co;2

Roebber, P. J., Grise, K. M., & Gyakum, J. R. (2023). The histories of well-documented maritime cyclones as portrayed by an automated tracking method. *Monthly Weather Review*, *151*(11), 2905–2924. https://doi.org/10.1175/Mwr-D-22-0287.1

Roebber, P. J., & Schumann, M. R. (2011). Physical processes governing the rapid deepening tail of maritime cyclogenesis. *Monthly Weather Review*, *139*(9), 2776–2789. https://doi.org/10.1175/Mwr-D-10-05002.1

Rogers, E., & Bosart, L. F. (1986). An investigation of explosively deepening oceanic cyclones. *Monthly Weather Review*, *114*(4), 702–718. https://doi.org/10.1175/1520-0493(1986)114<0702:AIOEDO>2.0.CO;2

Rogers, E., & Bosart, L. F. (1991). A diagnostic study of 2 intense oceanic cyclones. *Monthly Weather Review*, *119*(4), 965–996. https://doi.org/10.1175/1520-0493(1991)119<0965:Adsoti>2.0.Co;2

Saha, S., Moorthi, S., Pan, H.-L., Wu, X., Wang, J., Nadiga, S., et al. (2010). NCEP climate Forecast system reanalysis (CFSR) 6-hourly products, january 1979 to december 2010. [Dataset]. https://doi.org/10.5065/D69K487J. *Research Data Archive at the National Center for Atmospheric Research, Computational and Information Systems Laboratory*.

Saha, S., Moorthi, S., Wu, X., Wang, J., Nadiga, S., Tripp, P., et al. (2011). NCEP climate Forecast system version 2 (CFSv2) 6-hourly products. [Dataset]. https://doi.org/10.5065/D61C1TXF. *Research Data Archive at the National Center for Atmospheric Research, Computational and Information Systems Laboratory*.

Sanders, F., & Gyakum, J. R. (1980). Synoptic-dynamic climatology of the bomb. *Monthly Weather Review*, *108*(10), 1589–1606. https://doi.org/10.1175/1520-0493(1980)108<1589:Sdcot>2.0.Co;2

Seiler, C. (2019). A climatological assessment of intense extratropical cyclones from the potential vorticity perspective. *Journal of Climate*, *32*(8), 2369–2380. https://doi.org/10.1175/Jcli-D-18-0461.1

Seiler, C., & Zwiers, F. W. (2016a). How well do CMIP5 climate models reproduce explosive cyclones in the extratropics of the Northern Hemisphere? *Climate Dynamics*, *46*(3–4), 1241–1256. https://doi.org/10.1007/s00382-015-2642-x

Seiler, C., & Zwiers, F. W. (2016b). How will climate change affect explosive cyclones in the extratropics of the Northern Hemisphere? *Climate Dynamics*, *46*(11–12), 3633–3644. https://doi.org/10.1007/s00382-015-2791-y

Shaw, T. A., Baldwin, M., Barnes, E. A., Caballero, R., Garfinkel, C. I., Hwang, Y. T., et al. (2016). Storm track processes and the opposing influences of climate change. *Nature Geoscience*, *9*(9), 656–664. https://doi.org/10.1038/Ngeo2783

Spaete, P., Johnson, D. R., & Schaack, T. K. (1994). Stratospheric tropospheric mass-exchange during the presidents day storm. *Monthly Weather Review*, *122*(3), 424–439. https://doi.org/10.1175/1520-0493(1994)122<0424:Smedtp>2.0.Co;2

Strahl, J. L. S., & Smith, P. J. (2001). A diagnostic study of an explosively developing extratropical cyclone and an associated 500-hPa trough merger. *Monthly Weather Review*, *129*(9), 2310–2328. https://doi.org/10.1175/1520-0493(2001)129<2310:Adsoae>2.0.Co;2

Sun, Y., Zhu, Z. W., Yang, Y., & Lu, R. (2024). Decadal change in the connection between the Pacific-Japan pattern and the Indian Ocean SST basin mode. *Climate Dynamics*, *62*(5), 4281–4296. https://doi.org/10.1007/s00382-024-07132-2

Tamarin, T., & Kaspi, Y. (2016). The poleward motion of extratropical cyclones from a potential vorticity tendency analysis. *Journal of the Atmospheric Sciences*, *73*(4), 1687–1707. https://doi.org/10.1175/Jas-D-15-0168.1

Tsopouridis, L., Spengler, T., & Spensberger, C. (2021a). Smoother versus sharper gulf stream and kuroshio sea surface temperature fronts: Effects on cyclones and climatology. *Weather and Climate Dynamics*, *2*(4), 953–970. https://doi.org/10.5194/wcd-2-953-2021

Tsopouridis, L., Spensberger, C., & Spengler, T. (2021b). Characteristics of cyclones following different pathways in the Gulf Stream region. *Quarterly Journal of the Royal Meteorological Society*, *147*(734), 392–407. https://doi.org/10.1002/qj.3924

Tsopouridis, L., Spensberger, C., & Spengler, T. (2021c). Cyclone intensification in the Kuroshio region and its relation to the sea surface temperature front and upper-level forcing. *Quarterly Journal of the Royal Meteorological Society*, *147*(734), 485–500. https://doi.org/10.1002/qj.3929

Wang, C. C., & Rogers, J. C. (2001). A composite study of explosive cyclogenesis in different sectors of the North Atlantic. Part I: Cyclone structure and evolution. *Monthly Weather Review*, *129*(6), 1481–1499. https://doi.org/10.1175/1520-0493(2001)129<1481:Acsoec>2.0.Co;2

Wash, C. H., Hale, R. A., Dobos, P. H., & Wright, E. J. (1992). Study of explosive and nonexplosive cyclogenesis during fgge. *Monthly Weather Review*, *120*(1), 40–51. https://doi.org/10.1175/1520-0493(1992)120<0040:Soeanc>2.0.Co;2

Weijenborg, C., & Spengler, T. (2020). Diabatic heating as a pathway for cyclone clustering encompassing the extreme storm dagmar. *Geophysical Research Letters*, *47*(8). https://doi.org/10.1029/2019GL085777

Yang, Y., Zhu, Z. W., Shen, X. Y., Jiang, L. S., & Li, T. M. (2023). The influences of atlantic sea surface temperature anomalies on the ENSO-independent interannual variability of East Asian summer monsoon rainfall. *Journal of Climate*, *36*(2), 677–692. https://doi.org/10.1175/Jcli-D-22-0061.1

Yao, Y. L., Zhang, Y., Hodges, K. I., & Tamarin-Brodsky, T. (2023). Different propagation mechanisms of deep and shallow wintertime extratropical cyclones over the North pacific. *Journal of Climate*, *36*(23), 8277–8297. https://doi.org/10.1175/Jcli-D-22-0674.1

Yoshida, A., & Asuma, Y. (2004). Structures and environment of explosively developing extratropical cyclones in the northwestern Pacific region. *Monthly Weather Review*, *132*(5), 1121–1142. https://doi.org/10.1175/1520-0493(2004)132<1121:Saeoed>2.0.Co;2

Yoshiike, S., & Kawamura, R. (2009). Influence of wintertime large-scale circulation on the explosively developing cyclones over the western North Pacific and their downstream effects. *Journal of Geophysical Research*, *114*(D13). https://doi.org/10.1029/2009jd011820

Zhu, Y., & Newell, R. E. (1994). Atmospheric rivers and bombs. *Geophysical Research Letters*, *21*(18), 1999–2002. https://doi.org/10.1029/94gl01710